Bioorganic & Medicinal Chemistry 18 (2010) 822–829

Contents lists available at ScienceDirect

Bioorganic & Medicinal Chemistry

journal homepage: www.elsevier.com/locate/bmc

Novel and selective DNA methyltransferase inhibitors: Docking-based virtual screening and experimental evaluation

Dirk Kuck [a], Narender Singh [b], Frank Lyko [a], Jose L. Medina-Franco [b,*]

[a] Division of Epigenetics, Deutsches Krebsforschungszentrum, Im Neuenheimer Feld 580, 69120 Heidelberg, Germany
[b] Torrey Pines Institute for Molecular Studies, 11350 SW Village Parkway, Port St. Lucie, FL 34987, USA

ARTICLE INFO

Article history:
Received 17 September 2009
Revised 14 November 2009
Accepted 21 November 2009
Available online 27 November 2009

Keywords:
Cancer
DNA methyltransferases
Docking
Drug discovery
Epigenetics
Structure–activity relationships

ABSTRACT

The DNA methyltransferase (DNMT) enzyme family consists of four members with diverse functions and represents one of the most promising targets for the development of novel anticancer drugs. However, the standard drugs for DNMT inhibition are non-selective cytosine analogues with considerable cytotoxic side-effects that have been developed several decades ago. In this work, we conducted a virtual screening of more than 65,000 lead-like compounds selected from the National Cancer Institute collection using a multistep docking approach with a previously validated homology model of the catalytic domain of human DNMT1. Experimental evaluation of top-ranked molecules led to the discovery of novel small molecule DNMT1 inhibitors. Virtual screening hits were further evaluated for DNMT3B inhibition revealing several compounds with selectivity towards DNMT1. These are the first small molecules reported with biochemical selectivity towards an individual DNMT enzyme capable of binding in the same pocket as the native substrate cytosine, and are promising candidates for further rational optimization and development as anticancer drugs. The availability of enzyme-selective inhibitors will also be of great significance for understanding the role of individual DNMT enzymes in epigenetic regulation.

1. Introduction

DNA methylation plays an important role in mammalian development and disease.[1,2] In the human genome, about 4% of the cytosine residues are methylated in differentiated tissues. Methylation is mostly found at retroelements and other repetitive sequences, but also at promoters, genes, and intergenic regions.[3] Many human tumors showed widespread epigenetic changes when compared to their normal counterparts. This includes the hypermethylation of tumor suppressor genes, which is often associated with their transcriptional silencing.[4,5] As such, the functional relevance of epigenetic gene silencing to tumorigenesis[6] is similar to classical, genetic mutations. However, in contrast to genetic mutations, epigenetic mutations need to be actively maintained by DNA methylation and pharmacological inhibition of DNA methylation thus represents an attractive strategy for the reversion of epigenetic mutations.[7]

The human genome encodes four distinct DNA methyltransferases: DNMT1, DNMT2, DNMT3A, and DNMT3B. Of these, DNMT1 and DNMT3B constitute the major activities, which can be inferred from the strongly reduced DNA methylation levels of DNMT1; DNMT3B double knockout cell lines.[8] It has been shown that the inhibition of DNA methyltransferase activity can lead to demethylation and reactivation of epigenetically silenced tumor suppressor genes.[9] Thus, DNA methylation represents a central mechanism for mediating epigenetic gene regulation, and the development of DNA methyltransferase inhibitors provides novel opportunities for cancer therapy.[10,11]

Among the several known candidate DNA methyltransferase inhibitors, only two have been subjected to clinical development. These two drugs, 5-azacytidine and 5-aza-2′-deoxycytidine (decitabine) (Fig. 1), are nucleoside analogues which, after incorporation into DNA, cause covalent trapping and subsequent depletion of DNA methyltransferases.[12–14] The mode of action of azanucleosides probably involves several additional cellular pathways and their specificity is relatively low.[13] Consequently, these drugs are characterized by substantial cellular and clinical toxicity, which has driven the development of novel and more specific drugs. There is now an increasing number of substances that are reported to inhibit DNA methyltransferases.[15] Some of these compounds are approved drugs for other indications, for example, the antihypertensive drug hydralazine[16,17] or the local anesthetic

Abbreviations: DNMT, DNA methyltransferase; EGCG, (−)-epigallocatechin-3-gallate; HTVS, high-throughput virtual screening; MOE, Molecular Operating Environment; NCI, National Cancer Institute; RMS, root mean square; SAH, *S*-adenosylhomocysteine; SAM, *S*-adenosylmethionine; SP, standard precision; XP, extra precision.

* Corresponding author. Tel./fax: +1 772 345 4685.
E-mail address: jmedina@tpims.org (J.L. Medina-Franco).

0968-0896/$ - see front matter © 2009 Elsevier Ltd. All rights reserved.
doi:10.1016/j.bmc.2009.11.050

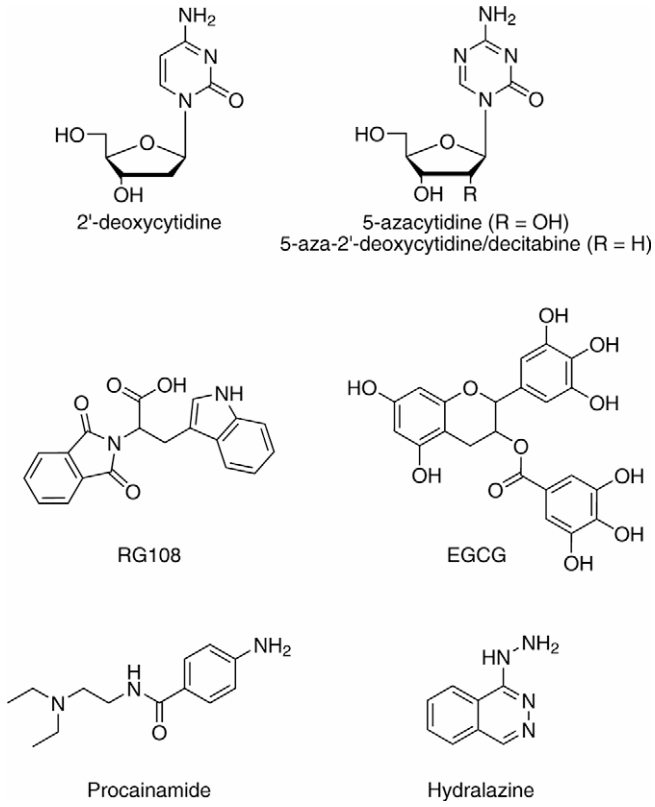

Figure 1. Chemical structures of selected DNMT1 inhibitors.

procainamide.[18] Other compounds are natural dietary components, like the main polyphenol compound from green tea, (−)-epigallocatechin-3-gallate (EGCG) or curcumin, the major component of the popular Indian curry spice turmeric.[19,20] Recently, SAH analogues presumably binding in the co-factor binding pocket, have also been reported as selective inhibitors towards DNMTs.[21,22] Until now, however, most compounds were identified fortuitously and there is only one rationally identified inhibitor of DNA methyltransferases, RG108.[23] Chemical structures of selected DNMT1 inhibitors are illustrated in Figure 1.

Molecular modeling and virtual screening of compound databases[24] are powerful computational approaches that are increasingly being used in drug discovery projects. These techniques are now commonly applied to help understand the binding mode of active compounds and identify new hits.[25–27] So far, only few molecular modeling studies with DNMT1 have been reported, proposing the binding mode of compounds such as EGCG,[19] decitabine, procaine, procainamide,[28] and curcumin.[20] Application of a docking-based virtual screening approach, with a validated homology model of DNMT1,[29] has also been published.[30] In that study, 1990 compounds in the Diversity Set available from the National Cancer Institute (NCI)[31] were the starting point for the virtual screening. Two of the top scoring compounds were tested experimentally showing activity both in vitro and in vivo, probably by binding into the DNMT1 catalytic pocket.[30]

In order to identify novel DNMT1 small molecule inhibitors with chemical scaffolds different from the currently known inhibitors, we now performed a multistep structure-based virtual screening of more than 65,000 lead-like compounds obtained from the NCI Open Database.[31] This is a large public database from which sample compounds can be obtained through the NCI/Developmental Therapeutics Program (DTP, see below). Since no crystallographic structure is available for the catalytic domain of DNMT1, structure-based screening was conducted using three docking programs with a previously validated homology model of the catalytic domain of human DNMT1.[29] A total of 13 top-ranked consensus hits, with calculated binding affinities more favorable than RG108 by all three docking programs were tested experimentally. Seven hits showed detectable DNMT1 inhibitory activity in a biochemical assay. The 13 compounds selected from virtual screening with DNMT1 were also assayed for DNMT3B inhibition. Notably, six out of the seven inhibitors appeared selective for DNMT1 and did not inhibit DNMT3B.

2. Results

At the time of this study, the NCI Open Database, as implemented in the ZINC database, consists of 260,071 compounds.[32] In order to focus the virtual screening on compounds that could be promising for further development, we selected a subset of lead-like compounds.[33,34] The selection was made based on properties and functional groups using the FILTER program[35] that reduced the initial NCI Database to a subset of 65,375 compounds (referred in this work as the NCI lead-like set). For FILTER we used the default parameters in the lead-like filter without further modifications (see Section 5 for details). The general workflow of the multistep docking approach implemented in this work is presented in Figure 2. Since no crystallographic structure of the catalytic site of human DNMT1 is available, we used an established homology model[29] in all steps of the virtual screening. The homology model used in this work has been successfully used for previous virtual screening[30] and modeling studies.[28] The amino acid sequence of the homology model of DNMT1 used in this study is shown in Figure S1 of Supplementary data. After selecting lead-like compounds,

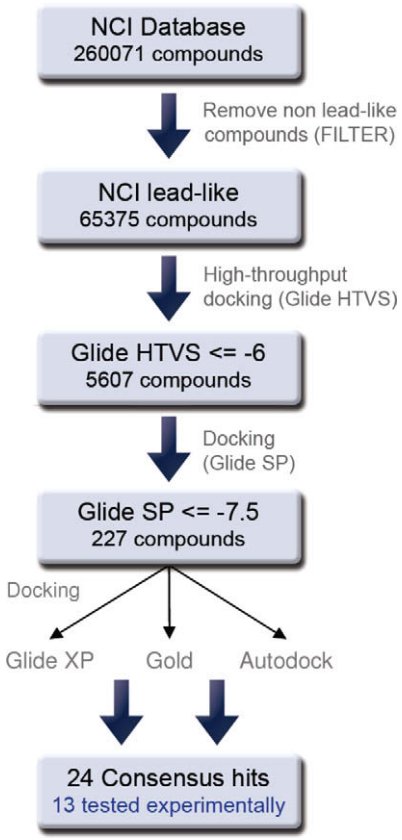

Figure 2. Flowchart of the multistep virtual screening strategy implemented in this work. After selecting lead-like compounds, the NCI Database was subsequently filtered with high-throughout docking and GLIDE SP. Top-ranked compounds were docked with GLIDE XP, GOLD and AUTODOCK. Consensus hits were identified and tested.

we employed a fast docking protocol to further filter the NCI lead-like set. As part of the screening, three docking programs were used. Consensus hits were selected and tested experimentally (Fig. 2). Details of the virtual screening approach and the biochemical characterization of selected compounds are presented below.

2.1. Virtual screening with DNMT1

The NCI lead-like set was prepared with LIGPREP[36] generating different protonation states and tautomers. The prepared set was docked into the DNMT1 active site using the GLIDE High-throughput Virtual Screening (HTVS) docking module.[37] Details of the dataset preparation with LIGPREP, protein preparation for docking and docking parameters, are presented in Section 5. Having targeted the 5,000 top scoring molecules for further analysis, we selected 5662 poses (5607 unique molecules) docked with GLIDE HTVS and a docking score $\leqslant -5.95$. These poses were further docked into the DNMT1 active site with GLIDE Standard Precision (SP). Finally, a total of 227 unique compounds (~200 poses plus molecules with GLIDE SP score $\leqslant -7.50$) were independently docked with GLIDE Extra Precision (XP), GOLD (GoldScore),[38] and AUTODOCK.[39] A total of 24 consensus compounds, with favorable docking scores by all three docking approaches, were identified out of which 13 were obtained for experimental testing. Consensus compounds were selected based on the corresponding docking scores of the prototypical DNMT inhibitor RG108 (Fig. 1) that was used as a reference (see Section 5). Consensus compounds showed more favorable docking scores than RG108 by all three docking programs. The chemical structures of the 13 compounds are shown in Figure 3A. The docking scores, docking ranks and selected lead-like properties are presented in Table S1 of Supplementary data. Most of the tested compounds were among the top 44 ranked compounds (out of the 227 docked) by any of the three docking programs. Only one molecule, NSC 319745 was ranked 65 by GLIDE XP. However, the same molecule was ranked 7 and 8 by AUTODOCK and GOLD, respectively (Table S1 in Supplementary data). The compounds selected from the virtual screening with DNMT1 were tested experimentally not only for DNMT1 inhibition but also for DNMT3B inhibition in order to assess biochemical selectivity.

2.2. Experimental testing with DNMT1 and DNMT3B

Standard biochemical assays for DNMT enzymes have not been established yet. In order to develop a biochemical in vitro methylation assay, human DNMT1 and DNMT3B enzymes were produced via baculovirus expression in insect cells. The identity and integrity of recombinant DNMT1 and DNMT3B, respectively, was confirmed by Coomassie staining and by Western blotting (data not shown). Enzymatic activity was determined by the incorporation of radioactive labeled methyl groups into hemimethylated or unmethylated oligonucleotides. Tritium labeled *S*-adenosylmethionine (SAM) was used as methyl group donor and the incorporation of radioactivity was quantitated by a scintillation counter. All compounds were obtained from the NCI Drug Synthesis and Chemistry Branch and were dissolved in DMSO to 50 mM stock solutions.

Table 1 shows the relative enzymatic activities of DNMT1 and DNMT3B in the presence of 100 μM test compound. Test compound concentrations had to be high, because the assay sensitivity and the low enzymatic activity required comparably high concentrations (800 nM) of enzyme. Compounds that caused an inhibition of more than 20% were scored as inhibitors (unspecific background signal was <10% for DNMT1 and <20% for DNMT3B). The results indicated selective inhibition of DNMT1 activity for six compounds (NSC 622444, 408488, 137546, 56071, 319745, 106084) and inhibition of both DNMT1 and DNMT3B for only one (NSC 14778). For comparisons, we also included a number of reference compounds in our assay (Table 1). RG108 and hydralazine showed a borderline inhibition of DNMT1 in this assay. We also tested NSC 348926, a compound chemically related to RG108 (Fig. 3B). Both molecules showed similar activity. Curcumin showed distinct inhibition of DNMT1 and a weaker inhibitory activity towards DNMT3B. SAH demonstrated a very efficient inhibition of both isoenzymes.

Dose–response curves and corresponding IC_{50} values were obtained for selected compounds and the results are summarized in Figure 4. In agreement with results in Table 1, NSC 14778 showed inhibition of DNMT1 and DNMT3B with IC_{50} values of 92 μM and 17 μM, respectively. In contrast, NSC 106084 only inhibited DNMT1. NSC 348926 was included as a negative control and revealed no inhibition for any of the isoenzymes (Fig. 4 and Table 1). SAH (*S*-adenosylhomocysteine) was used as a non-specific positive control and confirmed its efficient inhibition of both DNMT1 and DNMT3B (IC_{50} concentrations of 4 μM and 0.25 μM, respectively).

Taken together, our results thus establish novel DNMT inhibitors, and, for the first time, describe small molecules with biochemical selectivity towards individual DNMT enzymes capable of binding in the same pocket as the native substrate cytosine.

3. Discussion

The virtual screening approach using the homology model of the catalytic site of DNMT1 was successful in identifying several different scaffolds with DNMT1 inhibitory activity.[27] Notably, the seven compounds, that inhibit DNMT1, had a high docking rank, particularly with AUTODOCK (Table S1 in Supplementary data). For AUTODOCK the average docking rank of the seven compounds was 8.4 (standard deviation of 7.7) with a docking rank range of 1–23. For GLIDE XP and GOLD the corresponding average docking rank for the same compounds was 20.7 (standard deviation of 21.8) and 20.6, (standard deviation of 12.8), respectively. The docking rank range was 1–65 and 8–44 for GLIDE XP and GOLD, respectively. Interestingly both top two ranked compounds identified by AUTODOCK, NSC 106084 and 408488, showed detectable inhibitory activity in biochemical assays. The latter compound was also top ranked by GLIDE XP (Table S1 in Supplementary data).

Compounds NSC 14778, 622444, and 408488 are symmetric methylenedisalicylic acid derivatives with a diphenylmethane scaffold frequently found in approved drugs (Fig. 3).[40] As the substitution pattern in both phenyl rings changes from hydrogen in 14778, to chlorine in 622444, and methyl in 408488, the corresponding mean inhibitory activity for DNMT1 slightly decreases (mean 71%, 74%, and 78%, respectively; Table 1). In addition, a small change in the structure (e.g., substitution with a chlorine or methyl group) seemed to affect the isoenzyme selectivity. Other different scaffolds with selective DNMT1 inhibition are represented by compounds NSC 137546, 56071, 319745, and 106084. The structural diversity of these molecules represent an attractive potential to further explore different regions of the chemical space[41] with DNMT1 inhibitory activity and, in particular, selectivity towards individual DNMT enzymes.

We have included RG108 and hydralazine as reference compounds for the biochemical assay. Surprisingly, these compounds revealed only a borderline inhibition of DNMT1. This is probably related to the fact that most previous studies used crude protein extracts or other methyltransferase enzymes for their biochemical methylation assays.[17,20,30]

NSC 14778 or 5,5′-methylenedisalicylic acid, was among the most active compounds and is characterized by a distinct lead-like structure. In order to explore the putative interactions of NSC 14778 with DNMT1, the top-ranked binding modes found by GLIDE XP in complex with the binding pocket of the enzyme were sub-

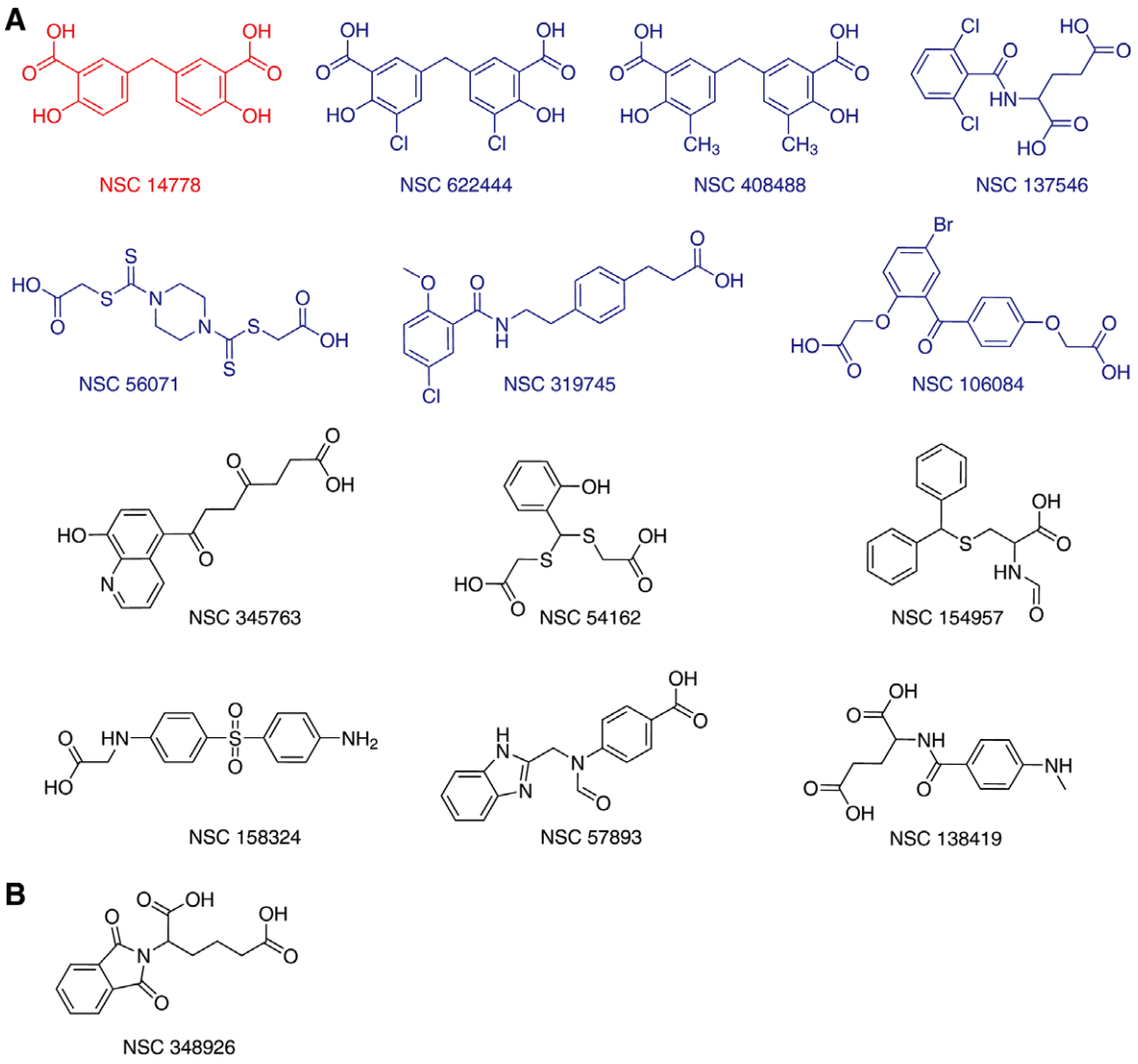

Figure 3. Chemical structures of compounds tested experimentally. (A) Compounds derived from the multistep docking approach. (B) Compound chemically related to RG108. Compounds selective for DNMT1 are highlighted in blue and the compound that inhibits both DNMT1 and DNMT3B is marked in red (see activity values in Table 1).

jected to full energy minimization using the MMFF94x force field implemented in MOE until the gradient 0.001 was reached. The default parameters implemented into the MOE's LigX application were used.[42] Figure 5 shows 3D and 2D representations of the optimized docked model of NSC 14778 with DNMT1. Similar optimized binding models were generated taking the top ranked poses predicted with GOLD and AUTODOCK. According to this binding model, residues that form the binding pocket of NSC 14778 are Pro86, Pro87, Cys88, Gln89, Ser92, Met94, Val130, Arg174, Thr320, Arg318, His321, Gly440, and Asn441 (see Fig. S1 of Supplementary data for residue numbering). A network of hydrogen bonds is predicted between one of the carboxylic acid groups of the ligand and the side chains of Arg174 and Arg318 (Fig. 5). A similar hydrogen bond network has been predicted between the phosphate group of 2′-deoxycytidine, and other related analogues, with the side chains of Arg174 and Arg318.[28] Interestingly, Arg174 plays an important role in the catalytic mechanism of DNA methylation.[28] An additional hydrogen bond is predicted between NSC 14778 and the backbone atoms of Pro86 and the catalytic Cys88. Similar interactions are observed in the optimized binding models of the related methylenedisalicylic acids NSC 622444 and 408488 (Fig. S2 in Supplementary data).

Figure 6A depicts a comparison of the optimized binding mode of NSC 14778 with a binding mode previously reported for 2′-deoxycytidine.[28] NSC 14778 adopts a similar binding mode as the nucleotide. Notably, one of the carboxylic groups of the virtual screening hit occupies the same binding pocket as the phosphate group of 2′-deoxycytidine (Fig. 6A) and is capable of making similar hydrogen bonds with the side chains of Arg174 and Arg318 (see Fig. 5). Of note, NSC 14778 lacks a cytosine ring. Comparison of the functional group placement between this compound and 2′-deoxycytidine (Fig. 6A), in addition to the analysis of the predicted binding mode within the catalytic site of DNMT1 (Fig. 5), indicates that formation of a covalent bond between NSC 14778 and the SH group of the catalytic cysteine is unlikely. Therefore, these observations suggest that NSC 14778 is a mechanism-independent inhibitor. Similar observations have been reported for RG108.[30] Figure 6B depicts a comparison of the optimized binding mode of NSC 14778, 137546, 56071, and 106084 within the catalytic site of DNMT1. Despite the very different scaffold, all four molecules adopt a comparable binding orientation. Of note, a carboxylic group present in three of the molecules occupies the same binding position making equivalent interactions with Arg174 and Arg318 (Fig. S2 in Supplementary data). Similar interactions have been predicted for RG108.[30] Taken together these

Table 1
Relative enzymatic activity of DNMT1 and DNMT3B in percent[a]

Compound	DNMT1	DNMT3B
NSC 14778	71(±3.1)	40(±0.7)
NSC 622444	74(±3.5)	104(±2.0)
NSC 408488	78(±3.8)	108(±1.9)
NSC 137546	73(±2.9)	106(±0.6)
NSC 56071	74(±2.7)	99(±1.0)
NSC 319745	66(±2.7)	128(0.7)
NSC 106084	78(±1.6)	96(±1.1)
NSC 345763	118(±6.1)	95(±0.4)
NSC 54162	98(±4.1)	99(±0.1)
NSC 154957	99(±4.4)	106(±0.6)
NSC 158324	97(±3.9)	92(±0.2)
NSC 57893	91(±4.3)	105(±2.8)
NSC 138419	91(±4.8)	104(±0.6)
NSC 348926[b]	85(±3.1)	99(±1.0)
RG108	83(±3.2)	110(±1,4)
Hydralazine	86(±3.7)	109(±2.1)
Curcumin	66(±0.4)	80(±1.3)
SAH	26(±0.6)	28(±0.2)

[a] Biochemical DNMT assay of NSC compounds against DNMT1 and DNMT3B. The relative enzymatic activity (in percent) is shown as the mean value of two measurements. Differences between individual measurements are indicated in percentage points. SAH (*S*-adenosylhomocysteine), curcumin, hydralazine and RG108 were used as reference compounds. All compounds were tested in a concentration of 100 μM against 800 nM of DNMT1 or DNMT3B. Compounds with an inhibition greater than 20% were scored as positive. Compounds selective for DNMT1 are highlighted in blue and compounds that inhibit both DNMTs are marked in red.
[b] This molecule was included because it is chemically related to RG108.

observations suggest that the binding modes obtained with docking for the active molecules with DNMT1 are reasonable and suggest that the carboxylate group present in all molecules may play a major role in the binding with DNMT1. It is hypothesized that with the modification of this carboxylate group, the activity of the molecules will significantly change.

As discussed above, the initial aim of this study was to identify novel small molecule DNMT1 inhibitors. Seven compounds with detectable inhibition of DNMT1 were identified by multistep virtual screening with a validated homology model of DNMT1 and experimental evaluation. In addition, we experimentally evaluated the selectivity of the active compounds. In biochemical assays with DNMT3B, six out of the seven compounds showed selectivity towards DNMT1. These findings open up the possibility to study the structural basis of selectivity.

Although a comprehensive molecular modeling study of the selectivity was out of the scope of this work, we report here hypotheses to explain our findings. The selectivity may be associated with the bigger catalytic site of DNMT1 as compared to the catalytic site DNMT3B which can lead to more favorable interactions with DNMT1. Since a detailed structural comparison of the binding modes is limited by the absence of a crystallographic structure of DNMT3B we constructed a homology model of the catalytic site of human DNMT3B using the crystal structure of DNMT3A[43] (PDB code 2QVR) as a template. Sequence alignment was done through ClustalW[44] and Prime,[45] a protein structure prediction suite from Schrödinger, LLC, was used for model building. The aligned sequence of query and template (Fig. S3 in Supplementary data) showed 81% homology and 96% similarity. Homology structure was built using this aligned template, taking into account the effects of solvent through various algorithms implemented in Prime. Missing query residues that did not match/align well with the template sequence were built using an ab initio procedure.[46] All the steric clashes were refined through minimization using OPLS2005 force field.[47] The final model showed a backbone RMSD of only 0.08 Å with the template structure. The sequence alignment of DNMT3B and DNMT1 is shown in Figure S4 in Supplementary data. This aligned sequence showed 12.3% identity and 37.2% similarity between the two enzymes. If the sequence alignment gap of 102 amino acids (Ser1394 to Leu1495) is not considered, these values are 16% identity and 48.5% similarity. An interesting observation was also made by superimposing the two structures, DNMT1 and DNMT3B. We observed that the side chain of residue Gln89 (or Gln1227 according to Supplementary data Fig. S1) is pointing in the interior of the binding side, whereas its equivalent Asn652 in DNMT3B points ~4 Å away from the binding pocket (see Supplementary data Fig. S5). Since docking of the six selective DNMT1 inhibitors into the catalytic site of DNMT3B with GLIDE XP showed consistently higher (less favorable) docking scores in DNMT3B as compared to the scores obtained with DNMT1 (data not shown), we propose that it may be due to the peculiar conformation of Gln89 in DNMT1. This residue acts as an important hydrogen bond donor to the docked compounds (Fig. S2 of Supplementary data) in DNMT1 binding site but not its equivalent Asn652 in DNMT3B. Further molecular modeling of these and other selective inhibitors discovered in our group with the homology models of DNMT1 and DNMT3B are on-going and will be published in due course.

4. Conclusions and perspectives

We are reporting for the first time small molecules with biochemical selectivity towards an individual human DNA methyltransferase enzyme. The identification of enzyme-selective inhibitors represents a major conceptual advance for future drug development and provides important tools for understanding the role of individual DNMT enzymes in epigenetic regulation.

Using a multistep docking approach of lead-like compounds with a homology model of the catalytic site of DNMT1, followed by experimental testing, we discovered seven new molecules with detectable DNMT1 inhibitory activity. The seven compounds had more favorable docking scores with DNMT1 than the reference compound RG108 by all three docking programs (GLIDE XP, GOLD, and AUTODOCK), and showed high docking ranks, particularly with AUTODOCK. Further experimental characterization of active compounds showed that six out of these seven inhibitors appeared selective for DNMT1 and did not inhibit the DNMT3B methyltransferase. The observed potency was comparably low for most test compounds, which we partially attribute to the high amount of protein used in the biochemical assay. The molecules identified in our study have diverse scaffolds, not previously reported for DNMT inhibitors, and represent excellent candidates for optimizing their inhibitory activity and selectivity. The findings obtained through this work represent the foundation for extensive molecular modeling studies to understand the structural basis of selectivity towards individual DNMTs.

5. Materials and methods

5.1. Database: lead-like selection and preparation

The NCI Open Database[31] with 260,071 compounds was obtained from ZINC.[32] The compound database was processed with FILTER,[35] version 2.0.1, to select a subset of lead-like compounds. We used the default parameters in the lead-like filter without further modifications. The resulting database, referred in this work as the NCI lead-like set, contained 65,375 compounds. For docking, different protonation states and tautomers were generated with LIGPREP,[36] version 2.2. This yielded a total of 90,653 structures.

5.2. Docking with GLIDE HTVS, SP, and XP

We employed the HTVS docking mode in GLIDE,[37] version 5.0, for a rapid structure-based filtering of the NCI lead-like set. This data set

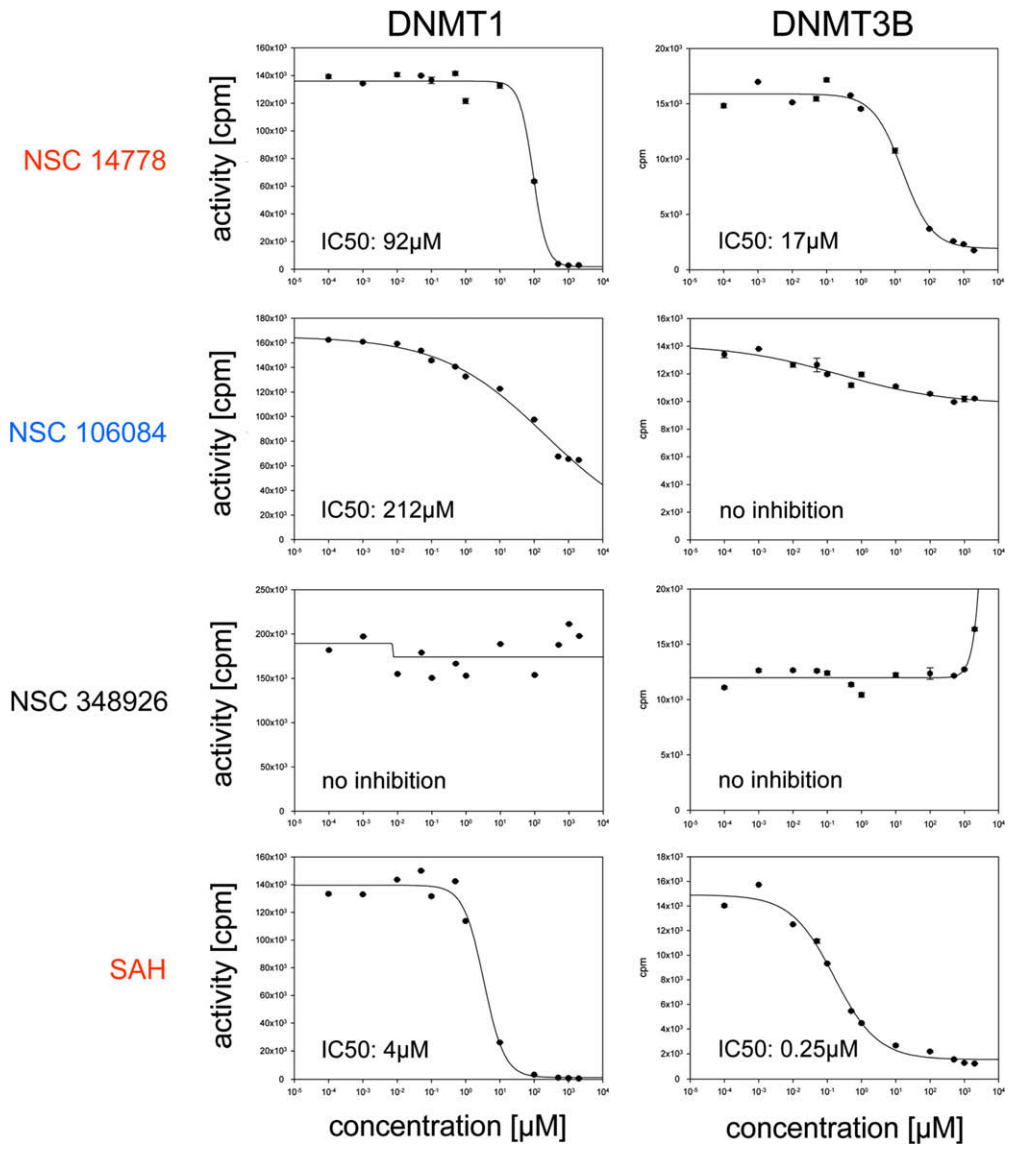

Figure 4. Dose–response plots for selected NSC compounds against DNMT1 or DNMT3B. The IC_{50} concentrations of selected compounds were determined by biochemical DNMT assays under identical conditions (500 nM enzyme, 0.7 μM AdoMet, 400 nM hemimethylated oligo). Each data point represents the mean ± SD of three measurements, and the data were analyzed by SigmaPlot version 10.0. Compounds selective for DNMT1 are highlighted in blue and compounds that inhibit both DNMTs are marked in red.

(previously prepared with LIGPREP) was docked with a validated homology model of the catalytic domain of human DNMT1 using the coordinates of the homology model published previously as a starting point.[29] The scoring grids were centered on the binding mode we reported recently for 2′-deoxycytidine using the same model of DNMT1.[28] We used the following bounding box size (in Å): $14 \times 10 \times 6$, that covers the catalytic pocket and part of the co-factor binding site. We used flexible docking with default parameters.

The top-ranked compounds with GLIDE HTVS were docked flexibly in a stepwise manner with GLIDE SP and XP (Fig. 2). We employed default parameters with the same receptor grids used with GLIDE HTVS.

5.3. Docking with GOLD

Selected compounds docked with GLIDE XP and AUTODOCK into the DNMT1 active site, were also docked with GOLD,[38] version 4.0 (Fig. 2). The binding site was defined by selecting all atoms within 10 Å of 2′-deoxycytidine (as found in the binding model we reported[28]) with the cavity detection mode turned on. Default parameters were used. A maximum of 10 docking runs per molecule were performed allowing early termination if top three solutions are within 1.5 Å RMS deviations of each other. Poses were evaluated with GoldScore. Cys88 was allowed to rotate freely during docking.[30]

5.4. Docking with AUTODOCK

Selected compounds docked with GLIDE XP and GOLD into the DNMT1 active site, were also docked with AUTODOCK,[39] version 3.0 (Fig. 2). We used the same grid maps (centered at the center of coordinates of docked 2′-deoxycytidine) and docking parameters reported for the docking of 2′-deoxycytidine and other compounds with the model of DNMT1.[28] The only modification was the number of docking runs that was set to 10 (previously 100) for faster virtual screening.

5.5. Compound selection for testing

A set of 227 compounds was docked with GLIDE XP, GOLD, and AUTODOCK (Fig. 2). In order to select consensus compounds for each list the following heuristic rule was applied:

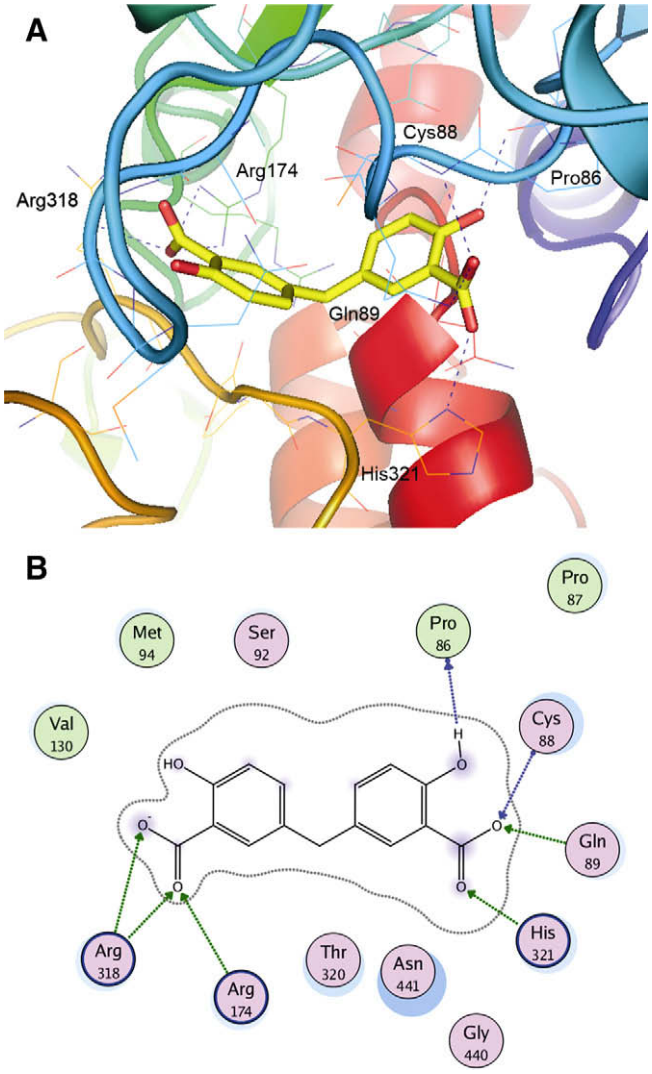

Figure 5. Optimized docking model of NSC 14778 with human DNMT1. (A) 3D representation showing selected amino acid residues. Hydrogen bonds are indicated with blue dashes. Hydrogen atoms are omitted for clarity; (B) 2D-interaction map displaying amino acid residues within 4.5 Å of the ligand. Green and blue arrows indicate hydrogen bonding to side chain and backbone atoms, respectively. Blue 'clouds' on ligand atoms indicate the solvent exposed surface area of ligand atoms. Light-blue 'halos' around residues indicate the degree of interaction with ligand atoms. The dotted contour reflects steric room for methyl substitution.

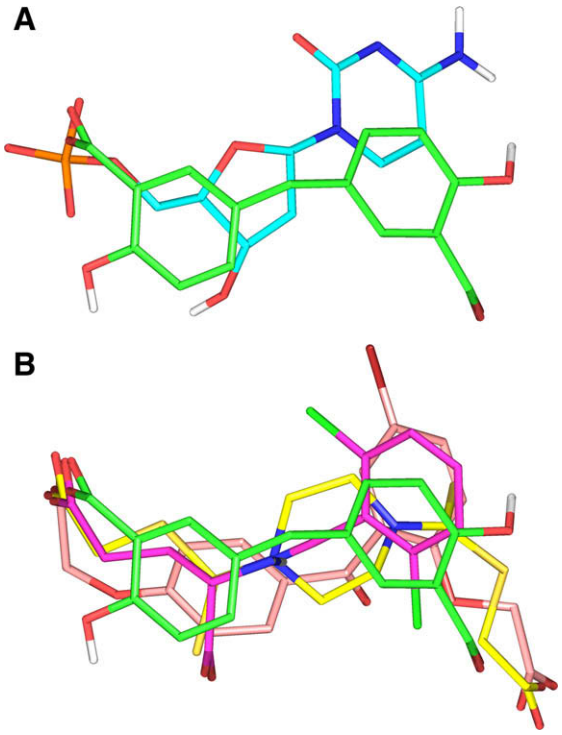

Figure 6. Comparison of the binding mode of NSC 14778 (carbon atoms in green) with the binding model of (A) 2′-deoxycytidine[28] (carbon atoms in cyan); (B) NSC 137546 (carbon atoms in magenta), 56071 (carbon atoms in yellow) and 106084 (carbon atoms in pink). Non-polar hydrogen atoms are omitted for clarity.

If GLIDE XP score $\leqslant T_{XP}$ and Autodock Docking Energy $\leqslant T_{ADE}$ and GoldScore $\geqslant T_{GS}$ then Consensus Hit

where T_{XP}, T_{ADE}, and T_{GS} are thresholds for GLIDE, AUTODOCK and GoldScore, respectively. We applied the following thresholds: $T_{XP} = -7.0$; $T_{ADE} = -13.99$; $T_{GS} = 62.0$. The thresholds were based on the docking scores obtained for RG108 (Table S1 in Supplementary data) that was taken as a reference. In total, we selected 24 consensus compounds from this list (Fig. 2). Out of the final 24 compounds identified from the multistep docking approach, 13 were obtained for experimental testing (Fig. 2).

5.6. Cloning and purification of human DNMT1 and DNMT3B

Generation of recombinant DNMT1 was described previously.[48] Recombinant baculoviruses encoding human DNMT3B fused to N-terminal 6xHis-tag were generated via the Bac-to-Bac baculovirus expression system (Invitrogen) according to manufacturer's protocol. The full-length DNMT3B gene was amplified by PCR and cloned into the FastbacHTc vector (Invitrogen). Identity and integrity of the DNMT3B gene was confirmed by plasmid sequencing. Sf9 cells were maintained in suspension culture with Ex-Cell 405 medium (Sigma, Taufkirchen, Germany) supplemented with gentamicin (50 μg/ml) and 5% fetal calf serum. Cells were grown in roller bottles and infected with a multiplicity of infection of 5–10 at a cell density of 1.0×10^6 cells/ml. The cells were kept at room temperature (RT) at 30 rpm and harvested 72 h after infection by centrifugation. The cell pellet was washed once with PBS. For protein purification, approximately 2.0×10^8 infected cells were resuspended in 15 ml of lysis buffer (150 mM KCl, 20 mM TrisCl pH 7.5, 1% NP40, 1 mM imidazole, 2 mM β-mercaptoethanol) supplemented with Protease Inhibitor Cocktail Complete Mini (Roche Applied Science). Cells were disrupted by sonication and centrifuged for 30 min at 10,000g at 4 °C. The supernatant was loaded onto NTA–agarose columns (Qiagen) equilibrated with buffer A (20 mM Na_2PO_4 pH 8.0; 10% glycerol, 500 mM NaCl, 40 mM imidazol). Columns were washed with 10 column volumes of buffer A and 10 volumes of buffer B (20 mM Na_2PO_4 pH 8.0; 10% glycerol, 100 mM NaCl). Proteins were eluted with five volumes of buffer C (20 mM Na_2PO_4 pH 8.0; 10% glycerol, 10 mM NaCl, 250 mM imidazole). The protein concentration of purified DNMT3B was determined by Bradford assay and verified by using Coomassie blue stained SDS/polyacrylamide gels and Western blotting using standard procedures.

5.7. Biochemical DNMT assay

DNA methylation assays were carried out in total reaction volume of 25 μl containing 0.4 μM hemimethylated or unmethylated oligonucleotide substrate purchased from MWG (upper strand: 5′-GATCGCXGATGCGXGAATXGCGATXGATGCGAT-3′, X = 5mC for

hemimethylated or X = C for unmethylated substrate, and lower strand: 5′-ATCGCATCGATCGCGATTCGCGCATCGGCGATC-3′), purified DNMT1 or DNMT3B protein, reaction buffer (100 mM KCL, 10 mM TrisCl pH 7.5, 1 mM EDTA) and BSA (1 mg/ml). All reactions were carried out at 37 °C in the presence of 0.7 μM [*methyl*-^{3}H] AdoMet (2.6 TBq/mmol, Perkin–Elmer). After 3 h the reaction was stopped by adding 10 μl 20% SDS and spotting of the whole volume onto DE81 cellulose paper. Filters were backed at 80 °C for 2 h and washed three times with cold 0.2 M NH_4HCO_3, three times with distillated water and once with 100% ethanol. After drying filters were transferred into Mini-Poly Q vial from Perkin–Elmer and 5 ml Ultima Gold LSC Cocktail was added per vial. Analysis was done in a Scintillation counter, each measurement was repeated once.

5.8. Compounds

All NSC compounds were obtained from the NCI/DTP Open Chemical Repository (http://dtp.cancer.gov), dissolved in DMSO and stored at −80 °C. *S*-Adenosylhomocysteine (SAH), hydralazine and RG108 were purchased by Sigma–Aldrich (Taufkirchen, Germany). Curcumin was purchased from Alfa Aesar (Karlsruhe, Germany).

Acknowledgments

Compounds tested were kindly supplied by the National Cancer Institute, Drug Synthesis and Chemistry Branch. We thank Dr. Karina Martínez-Mayorga for helpful discussions and critically reading the manuscript. The assistance of Page Hoskins is also acknowledged. We are grateful to OpenEye Scientific Software, Inc. for providing the FILTER program. This work was supported by the State of Florida, Executive Office of the Governor's Office of Tourism, Trade, and Economic Development.

Supplementary data

Supplementary data associated with this article can be found, in the online version, at doi:10.1016/j.bmc.2009.11.050.

References and notes

1. Klose, R. J.; Bird, A. P. *Trends Biochem. Sci.* **2006**, *31*, 89.
2. Jones, P. A.; Baylin, S. B. *Nat. Rev. Genet.* **2002**, *3*, 415.
3. Lister, R.; Pelizzola, M.; Dowen, R. H.; Hawkins, R. D.; Hon, G.; Tonti-Filippini, J.; Nery, J. R.; Lee, L.; Ye, Z.; Ngo, Q. M.; Edsall, L.; Antosiewicz-Bourget, J.; Stewart, R.; Ruotti, V.; Millar, A. H.; Thomson, J. A.; Ren, B.; Ecker *J. R. Nature* **2009**, *462*, 315.
4. Esteller, M. *Nat. Rev. Genet.* **2007**, *8*, 286.
5. Jones, P. A.; Baylin, S. B. *Cell* **2007**, *128*, 683.
6. Baylin, S. B.; Ohm, J. E. *Nat. Rev. Cancer* **2006**, *6*, 107.
7. Goll, M. G.; Bestor, T. H. *Annu. Rev. Biochem.* **2005**, *74*, 481.
8. Rhee, I.; Bachman, K. E.; Park, B. H.; Jair, K. W.; Yen, R. W.; Schuebel, K. E.; Cui, H.; Feinberg, A. P.; Lengauer, C.; Kinzler, K. W.; Baylin, S. B.; Vogelstein, B. *Nature* **2002**, *416*, 552.
9. Egger, G.; Liang, G.; Aparicio, A.; Jones, P. A. *Nature* **2004**, *429*, 457.
10. Svedruzic, Z. M. *Curr. Med. Chem.* **2008**, *15*, 92.
11. Yu, N.; Wang, M. *Curr. Med. Chem.* **2008**, *15*, 1350.
12. Liu, K.; Wang, Y. F.; Cantemir, C.; Muller, M. T. *Mol. Cell. Biol.* **2003**, *23*, 2709.
13. Stresemann, C.; Lyko, F. *Int. J. Cancer* **2008**, *123*, 8.
14. Schermelleh, L.; Spada, F.; Easwaran, H. P.; Zolghadr, K.; Margot, J. B.; Cardoso, M. C.; Leonhardt, H. *Nat. Methods* **2005**, *2*, 751.
15. Lyko, F.; Brown, R. J. *Natl. Cancer Inst.* **2005**, *97*, 1498.
16. Segura-Pacheco, B.; Trejo-Becerril, C.; Pérez-Cárdenas, E.; Taja-Chayeb, L.; Mariscal, I.; Chávez, A.; Acuña, C.; Salazar, A. M.; Lizano, M.; Dueñas-González, A. *Clin. Cancer Res.* **2003**, *9*, 1596.
17. Segura-Pacheco, B.; Pérez-Cárdenas, E.; Taja-Chayeb, L.; Chávez-Blanco, A.; Revilla-Vázquez, A.; Benítez-Bribiesca, L.; Dueñas-González, A. *J. Transl. Med.* **2006**, *4*, 32.
18. Lee, B. H.; Yegnasubramanian, S.; Lin, X. H.; Nelson, W. G. *J. Biol. Chem.* **2005**, *280*, 40749.
19. Fang, M. Z.; Wang, Y.; Ai, N.; Hou, Z.; Sun, Y.; Lu, H.; Welsh, W.; Yang, C. S. *Cancer Res.* **2003**, *63*, 7563.
20. Liu, Z. F.; Xie, Z. L.; Jones, W.; Pavlovicz, R. E.; Liu, S. J.; Yu, J. H.; Li, P. K.; Lin, J. Y.; Fuchs, J. R.; Marcucci, G.; Li, C. L.; Chan, K. K. *Bioorg. Med. Chem. Lett.* **2009**, *19*, 706.
21. Isakovic, L.; Saavedra, O. M.; Llewellyn, D. B.; Claridge, S.; Zhan, L.; Bernstein, N.; Vaisburg, A.; Elowe, N.; Petschner, A. J.; Rahil, J.; Beaulieu, N.; Gauthier, F.; MacLeod, A. R.; Delorme, D.; Besterman, J. M.; Wahhab, A. *Bioorg. Med. Chem. Lett.* **2009**, *19*, 2742.
22. Saavedra, O. M.; Isakovic, L.; Llewellyn, D. B.; Zhan, L.; Bernstein, N.; Claridge, S.; Raeppel, F.; Vaisburg, A.; Elowe, N.; Petschner, A. J.; Rahil, J.; Beaulieu, N.; MacLeod, A. R.; Delorme, D.; Besterman, J. M.; Wahhab, A. *Bioorg. Med. Chem. Lett.* **2009**, *19*, 2747.
23. Brueckner, B.; Lyko, F. *Trends Pharmacol. Sci.* **2004**, *25*, 551.
24. Scior, T.; Bernard, P.; Medina-Franco, J. L.; Maggiora, G. M. *Mini-Rev. Med. Chem.* **2007**, *7*, 851.
25. Jorgensen, W. L. *Science* **2004**, *303*, 1813.
26. Guido, R. V. C.; Oliva, G.; Andricopulo, A. D. *Curr. Med. Chem.* **2008**, *15*, 37.
27. Muegge, I. *Mini-Rev. Med. Chem.* **2008**, *8*, 927.
28. Singh, N.; Dueñas-González, A.; Lyko, F.; Medina-Franco, J. L. *ChemMedChem* **2009**, *4*, 792.
29. Siedlecki, P.; Boy, R. G.; Comagic, S.; Schirrmacher, R.; Wiessler, M.; Zielenkiewicz, P.; Suhai, S.; Lyko, F. *Biochem. Biophys. Res. Commun.* **2003**, *306*, 558.
30. Siedlecki, P.; Boy, R. G.; Musch, T.; Brueckner, B.; Suhai, S.; Lyko, F.; Zielenkiewicz, P. *J. Med. Chem.* **2006**, *49*, 678.
31. Developmental Therapeutics Program, National Cancer Institute. http://dtp.cancer.gov (accessed Sep 2009).
32. Irwin, J. J.; Shoichet, B. K. *J. Chem. Inf. Model.* **2005**, *45*, 177.
33. Charifson, P. S.; Walters, W. P. *J. Comput.-Aided Mol. Des.* **2002**, *16*, 311.
34. Oprea, T. I.; Bologa, C.; Olah, M. In *Virtual Screening in Drug Discovery*; Alvarez, J., Shoichet, B., Eds.; Taylor & Francis: Boca Raton, 2005; pp 89–106.
35. FILTER, version 2.0.1; OpenEye Scientific Software Inc.: Santa Fe, NM. http://www.eyesopen.com (accessed Sep 2009).
36. LIGPREP, version 2.2, Schrödinger, LLC, New York, NY, 2005.
37. GLIDE, version 5.0, Schrödinger, LLC, New York, NY, 2008.
38. Jones, G.; Willett, P.; Glen, R. C.; Leach, A. R.; Taylor, R. *J. Mol. Biol.* **1997**, *267*, 727.
39. Morris, G. M.; Goodsell, D. S.; Halliday, R. S.; Huey, R.; Hart, W. E.; Belew, R. K.; Olson, A. J. *J. Comput. Chem.* **1998**, *19*, 1639.
40. Singh, N.; Guha, R.; Giulianotti, M. A.; Pinilla, C.; Houghten, R. A.; Medina-Franco, J. L. *J. Chem. Inf. Model.* **2009**, *49*, 1010.
41. Medina-Franco, J. L.; Martinez-Mayorga, K.; Giulianotti, M. A.; Houghten, R. A.; Pinilla, C. *Curr. Comput.-Aided Drug Des.* **2008**, *4*, 322.
42. Molecular Operating Environment (MOE), version 2008.10; Chemical Computing Group Inc.: Montreal, Quebec, Canada. http://www.chemcomp.com (accessed Sep 2009).
43. Jia, D.; Jurkowska, R. Z.; Zhang, X.; Jeltsch, A.; Cheng, X. *Nature* **2007**, *449*, 248.
44. Chenna, R.; Sugawara, H.; Koike, T.; López, R.; Gibson, T. J.; Higgins, D. G.; Thompson, J. D. *Nucleic Acids Res.* **2003**, *31*, 3497.
45. Prime, version 2.1.108, Schrödinger LLC, New York, NY, 2009.
46. Jacobson, M. P.; Pincus, D. L.; Rapp, C. S.; Day, T. J.; Honig, B.; Shaw, D. E.; Friesner, R. A. *Proteins* **2004**, *55*, 351.
47. Kaminski, G. A.; Friesner, R. A.; Tirado-Rives, J.; Jorgensen, W. L. *J. Phys. Chem. B* **2001**, *105*, 6474.
48. Castellano, S.; Kuck, D.; Sala, M.; Novellino, E.; Lyko, F.; Sbardella, G. *J. Med. Chem.* **2008**, *51*, 2321.